17th World Conference on Earthquake Engineering, 17WCEE
Sendai, Japan - September 13th to 18th 2020

ANALYSIS AND SYNTHESIS OF SURFACE WAVES IN SEDIMENTARY BASINS

K.C. Meza-Fajardo(1), H. Aochi(2), A.S. Papageorgiou(3)

(1) Researcher, BRGM, k.mezafajardo@brgm.fr

(2) Researcher, BRGM, h.aochi@brgm.fr

(3) Professor, University of Patras, papaga@upatras.gr

Abstract

Basin induced surface waves are generated when seismic energy (usually in the form of body waves) is impinging on sediments which form a basin/valley. Such locally induced surface waves cause significant elongation of the duration of strong ground motion, especially in the intermediate and long period range. Analysis and simulation of such locally induced surface waves have been the subject of numerous investigations. Despite the large number of such investigations, we still do not have a workable model for predicting/synthesizing long period strong ground motion given a few basic earthquake source parameters (e.g. magnitude) and gross geological structure. The purpose of the present investigation is to develop such a model.

We consider for analysis two well instrumented sedimentary basins (e.g. the Nagoya and Kanto basins in Japan) which have recorded earthquake events with a range of magnitudes. The recorded ground motions are analyzed so as to separate surface waves from body waves. Prograde and retrograde Rayleigh waves are identified. For this identification/separation we make extensive use of the 'Normalized Inner Product' (NIP) method. As a byproduct of this separation is the evaluation the 'group-delay' spectrum, which is one of the two important input elements for the stochastic synthesis of long-period ground motion, the other element being the amplification (primarily in the long period range) of the incoming seismic energy due to the presence of the sediments. The obvious questions are: 'Given a site in a basin, how stable are the group-delay spectrum and amplification function for that site?'; 'Which factors (e.g. earthquake magnitude, azimuthal direction, etc.) affect the group-delay spectrum and amplification function at a site, and how?'; 'Are the group delay spectrum and amplification function predictable in terms of basic source parameters and a basic knowledge of the gross geological structure of the basin?'. Our investigation aims at addressing, and eventually, answering these questions.

Keywords: surface waves, stochastic model, group delay spectrum

1. Introduction

Recent seismic events have allowed the observation of the effects of long-period motions on large-scale structures, such as high-rise buildings, industrial facilities, and long-span suspension bridges. In most cases long-period ground motions consist primarily of surface waves, which are generated by conversion of incident body wave energy on sedimentary deposits. Distinctive examples of well documented basin-induced surface waves in the recent past were the motions recorded on the Mexico Valley during the 1985 Michoacán earthquake and the motions recorded on the Po Plain during the 2012 Emilia earthquake in Northern Italy. Many studies in Japan focusing on the Kanto and Osaka basin (*e.g.*, [1], [2]) have observed late-arriving surface waves which have been attributed to a generation process at the edges of the respective sedimentary basins.

In this work, we study surface waves propagating through sedimentary basins that have recorded major recent events. We consider the Nagoya and Kanto basins in Japan, both of them instrumented with dense strong motion networks. The Nobi basin (also referred to as the Nobi plain) in Japan is a sediment filled valley extending over an area of about 1800 square kilometers. The city of Nagoya, being the fourth-most-populous urban area in Japan with more than 2 million people, is located on the basin. The Kanto basin, where Tokyo, the capital of Japan is located, has been the subject of many studies that have focused on basin effects.

In the present work, exploiting a recently proposed method (referred to as the Normalized Inner Product – NIP for short) [3], we analyze the seismic wave-field, propagating in the abovementioned basins. We first identify and separate the various types of surface waves and then we proceed to quantify them in terms of their amplitude and duration. For the two basins we analyze the complex wave-field that was generated by the megathrust 2011 Tohoku earthquake, and two smaller earthquake events, the Chuetsu and the Chuetsu-oki events. With our investigation, we attempt to follow the 'flow' of seismic energy as it approaches just outside the basins, and then how it evolves once inside the basin. We highlight the differences in basin response considering their different structures and the events exciting them. We present quantitative analyses both in space and time of the extracted surface waves and the distribution of their features throughout the basins.

2. The Nobi basin

The Nobi basin, located in the central part of Japan (see Figure 1), is a basin with a maximum depth of 3 km composed of Alluvial, Pleistocene and Tertiary strata. Figure 1b shows the bedrock depth of the basin, indicated by the depth of the layer corresponding to Vs=2700 km/s, retrieved from the 3D national deep structure model of the National Research Institute for Earth Science and Disaster Resilience (NIED) of Japan [4]. We then consider three well-known major events, the great 2011 Tohoku earthquake and the 2004 Chuetsu and 2007 Chuetsu-oki earthquakes. Their source parameters are listed in Table 1, where we note that the Chuetsu and Chuetsu-oki earthquakes have the same magnitude and similar focal depth. In addition of being closely located, the focal mechanisms for these two earthquakes can be considered virtually identical.

At the K-NET stations, ground motions are recorded by high-resolution accelerometers. In this analysis we identify and extract Rayleigh waves based on their characteristic elliptical polarization, which requires that we work with displacement histories. These displacement histories were derived from the recorded acceleration histories, by band-pass filtering between 0.05 and 20 Hz, and then integrating in time twice. We implement the filtering technique presented in [3], [5] to identify and extract surface waves from three-component seismograms. Each station is processed independently, and assuming that the surface wave energy dominating the seismogram corresponds to retrograde Rayleigh waves, as it is the mode most commonly observed in ground motion recordings. Prograde Rayleigh waves are also investigated, especially when the direction of retrograde wave propagation among several stations cannot be verified.

In Figure 2 we show the Rayleigh waves extracted at the Nobi basin for the three events in the range 0.1-0.5 Hz. We observe that in the three events Rayleigh waves are identified before the seimic energy propagates through the basin. During the Chuetsu and the Chuetsu-oki earthquakes the Rayleigh waves arriving to the base propagate towards the Southwest, whereas during the Tohoku earthquake, the arriving Rayleigh

waves propagate to the Northwest. The difference in basin response is illustrated in Figure 2, where we can observe that in the case of the Tohoku earthquake the Rayleigh waves are diffracted by the basin, and thus they lose coherency as they arrive to the western-most stations. This effect is not observed during the Chuetsu and Chuetsu-oki events. Also, during the Tohoku event, we observe an elongated duration of the Rayleigh waves at station AIC003 which is located in a deep part of the basin. The Rayleigh waves for the Tohoku earthquake have similar central frequency but apparently the incident seismic field has a broader frequency content, as compared to the almost monochromatic incident wave-field in the case of the Chuetsu and Chuetsu-oki earthquakes.

(a) (b)

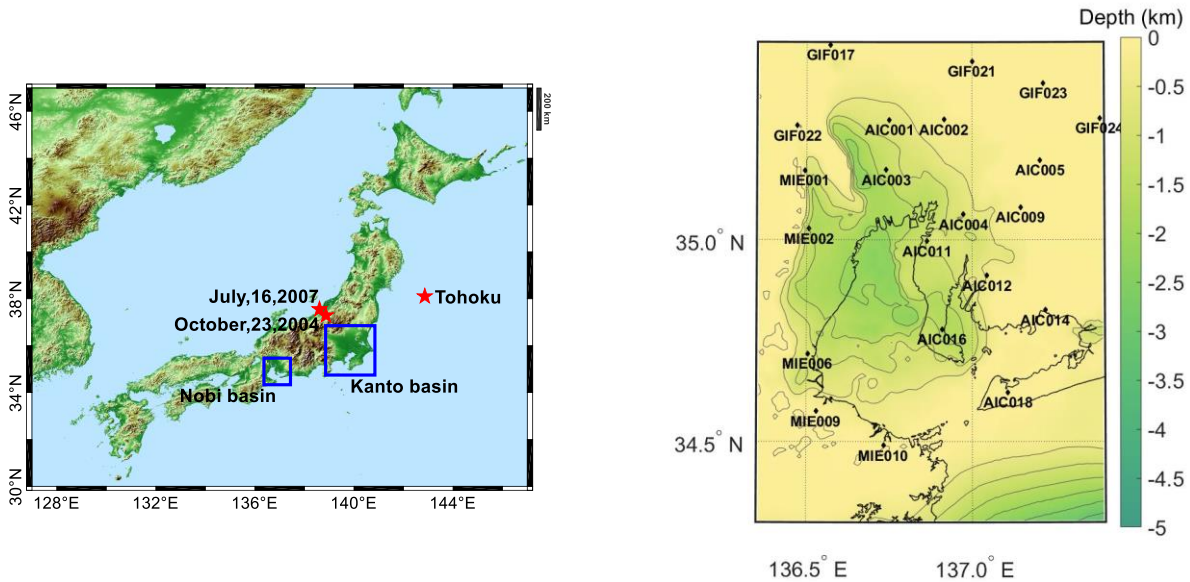

Figure 1. (a) Location of the Nobi and Kanto basins (indicated by the squares), and locations of the epicenters of the events (indicated by stars), considered in this study. (b) Spatial distribution of strong motion K-NET stations in the Nobi basin. The contours plots indicate the depth corresponding to Vs=2700 m/s.

Table 1. Earthquake events considered for surface wave analysis in Nobi and Kanto basins. Earthquake information is based on the catalogue of Japan Meteorological Agency. Time is local time (JST).

Name	Event time	Magnitude M_{JMA}	Latitude	Longitude	Depth (Km)	Note
Chuetsu	2004/10/23 17:56:00	6.8	37.291	138.867	13	Crustal reverse faulting
Chuetsu-oki	2007/07/16 10:13:00	6.8	31.557	136.608	17	Crustal reverse faulting
Tohoku	2011/03/11 14:46:00	9.0	38.103	142.86	24	Subduction

For the three events considered, we conclude that the identified Rayleigh waves are not generated by the basin, even though they interact with it in some cases. However, it is our interest to quantify those effects and observe how they relate to the group delay spectrum (GDS). The GDS is a function of frequency that provides the time the peak of the envelope of each frequency arrives to the station. In order to quantify the characteristics of the GDS in a simple manner, we measure the time delay of the central frequency of the extracted waves (denoted by t_{de}) with respect to the time delay of a higher frequency (denoted by t_{rf}), as follows:

$$t_{dr} = t_{de} - t_{rf} \tag{1}$$

where t_{dr} is the relative time delay and the higher frequency selected for our study is 3 Hz.

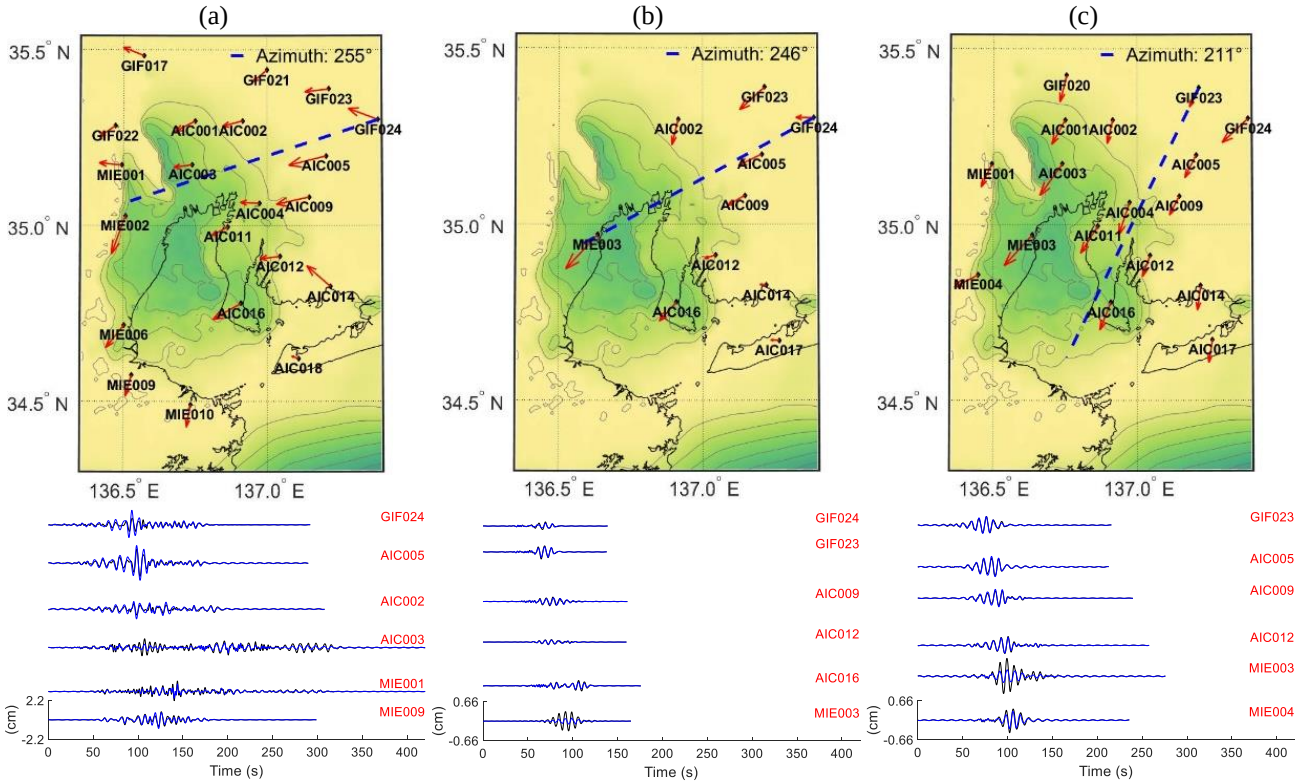

Figure 2. Rayleigh waves extracted at the Nobi basin during (a) the Tohoku (b) the Chuetsu, and (c) the Chuetsu-oki earthquake. Directions of polarization are shown on the top panels. The intermittent straight line, on the top panels, indicates the direction of maximum energy averaged over all stations shown in the figure. On the bottom panels, plots of horizontal and vertical components of extracted wave trains. The time-history of the vertical component is shifted to show there is a pi/2 shift with respect to the time-history of the horizontal component.

Figure 3 shows the relative time delay computed for the Rayleigh waves of Figure 2, at the central frequencies also shown in Figure 3. Here we use the term '*central frequency*' to refer to the frequency corresponding to the maximum amplitude of the Stockwell Transform [6] of the extracted wave. Figure 3 clearly illustrates that in the case of the Tohoku event the range of central frequencies of Rayleigh waves is higher than those of the other two events; in the latter two cases the central frequencies remain below 0.15 Hz. Figures 3(d)-(f) do not indicate a regular pattern for the distribution of the relative time delay in the basin, however we can observe that the range of this parameter for the Chuetsu and Chuetsu-oki earthquakes is very similar (between 10 and 30 s) whereas during the Tohoku earthquake the range is much larger (from 5 to 80 s). This indicates that during Tohoku earthquake the Rayleigh waves were better separated (arrived much later) from the rest of the waves. We attribute this to the larger epicentral distance of the Tohoku earthquake, and to the considerably larger size of the radiating source, as compared to the two Chuetsu events. We also observe that during the Tohoku earthquake, the relative time delay is reduced as the waves propagate through the basin, arguably due to diffraction.

Besides, in order to quantify the amplitude increase due to the presence of Rayleigh waves, in Figure 4 we show the ratio of the amplitude of the S-transform of the total signal with respect to the amplitude of the S-transform of the signal without the surface waves. Both amplitudes correspond to the central frequencies shown in Figure 3. To minimize interference with other type of surface waves (Love waves for example), we use the vertical component to measure the normalized amplitude. Once again, we observe that the ranges of normalized amplitude are similar for the two Chuetsu earthquakes. For the Tohoku earthquake the range of normalized amplitude is smaller, the amplitude of the Rayleigh waves can be up to six times the amplitude of the body waves, at the central frequency. Let us note that these normalized amplitudes are not stronger at stations inside the basin, because these Rayleigh waves are not basin generated.

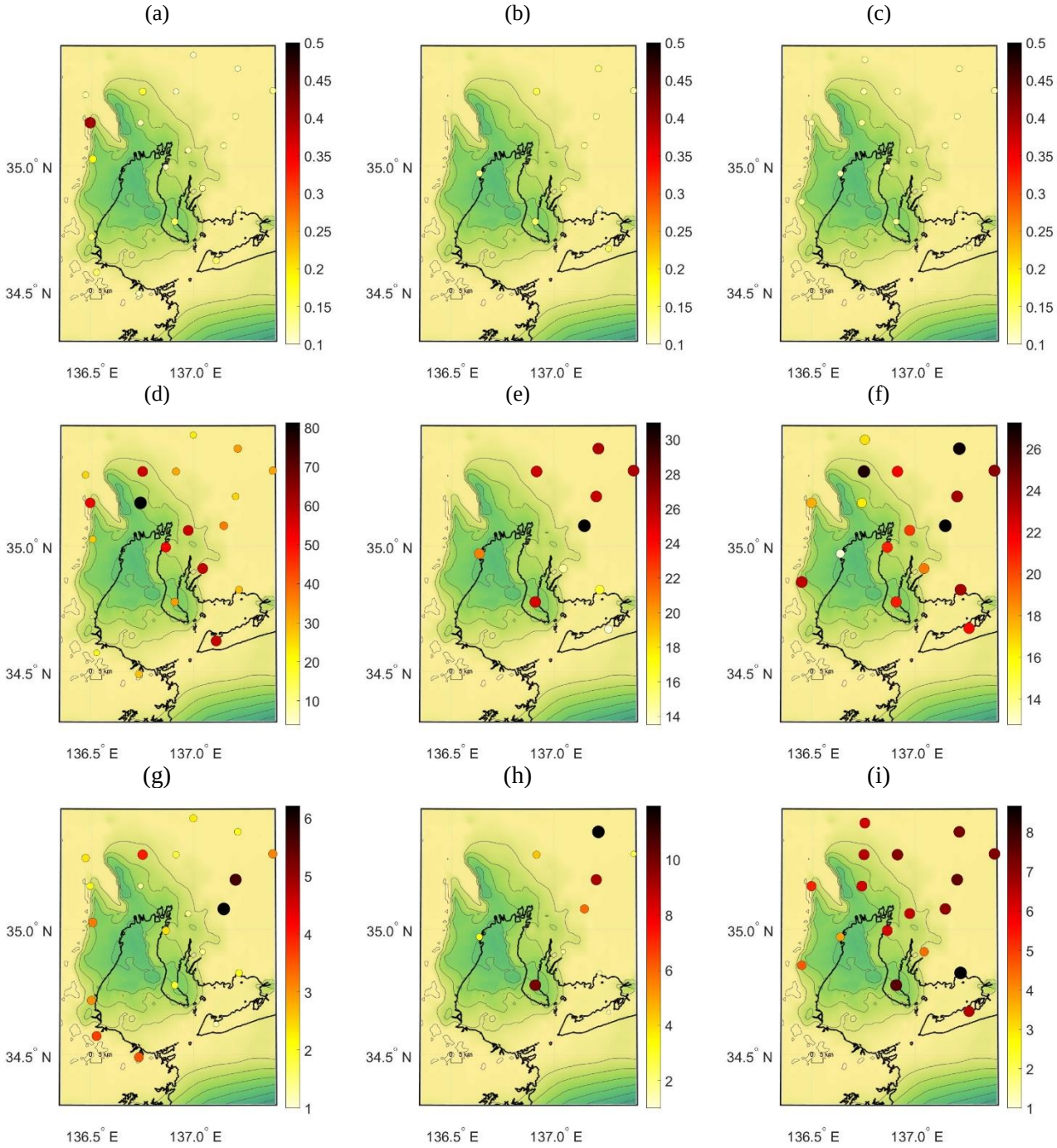

Figure 3. Rayleigh waves extracted at the Nobi basin. (a), (b) and (c) Central frequency (Hz) during the Tohoku, the Chuetsu and the Chuetsu-oki earthquake, respectively. (d), (e) and (f) Relative time delay during the Tohoku, the Chuetsu and the Chuetsu-oki earthquake, respectively. (g), (h) and (i) Normalized amplitude during the Tohoku, the Chuetsu and the Chuetsu-oki earthquake, respectively.

3. The Kanto basin

The well-known Kanto basin is a deep and complex sedimentary basin with an inland bedrock depth as large as 4 km under the Chiba prefecture. Figure 5 shows the bedrock depth of the two basins, indicated by the depth of the layer corresponding to Vs=2700 km/s, retrieved from the 3D national deep structure model of NIED. The geometry of the Kanto basin includes deposits in the form of several elongated branches. As the maximum

depths of the Nobi and Kanto basins differ significantly when compared to each other, and their locations with respect to the epicenters also differ, we can expect different basin responses to the incoming wave fields. We analyze the response of the Kanto basin considering the same three earthquakes listed in Table 1.

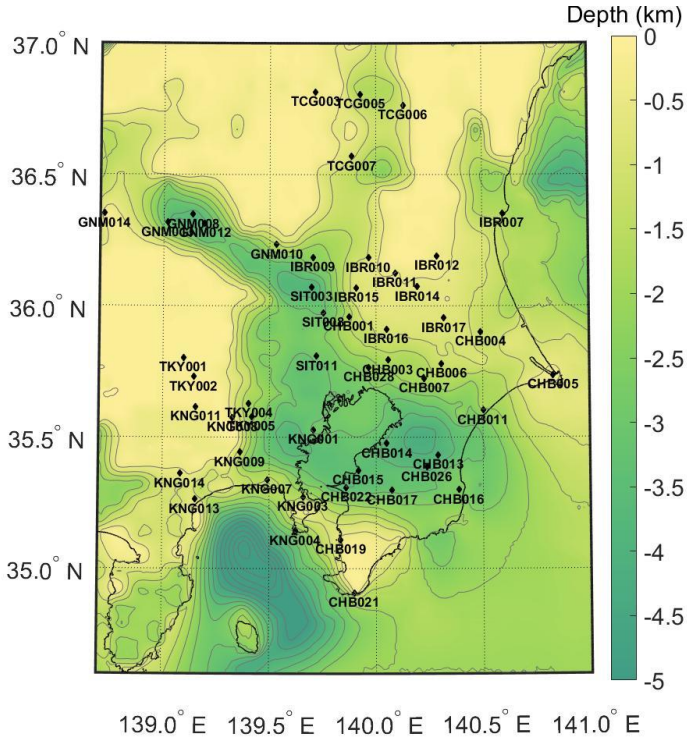

Figure 5. Spatial distribution of strong motion K-NET stations in the Kanto basin. The contours plots indicate the depth corresponding to Vs=2700 m/s.

For the Kanto basin we focus in the same range of frequencies (0.1-0.5 Hz) as in the Nobi basin. For the three events, we found that Rayleigh waves identified in the western regions of the basin are retrograde, and those identified on the central (Tokyo) and south-eastern (Chiba) region are prograde. In figure 6 we present the comparison of *retrograde* waves propagating in the western Gunma-Saitama region. For the Tohoku earthquake we observe that Rayleigh waves are diffracted at the deeper parts of the region, and that they therefore lose coherency. In the case of the two Chuetsu earthquakes, we observe a low-frequency pulse propagating on the northern edge of the elongated region of sediments, losing coherency in the deepest parts of the region as well.

Figure 7 we present the extracted *prograde* Rayleigh waves in the Tokyo bay area. We observe more coherence among the extracted waves because the inter-station distance in this region is smaller than that of the Gunma-Saitama region. The direction of propagation of the Rayleigh waves during the two Chuetsu earthquakes is very similar, as well as the extracted waveforms, and in particular, their duration. Not surprisingly, for the Tohoku earthquake the absolute amplitudes and the duration of the waveforms are much larger.

In Figure 8 we show the central frequency with corresponding relative time delay and normalized amplitude of the extracted waves in the Gunma-Saitama region. For the three events we observe that the central frequencies are in the range 0.15-0.30 Hz, and also a similar range of the relative time delay (10-60 s). However, for the Tohoku earthquake a higher number of stations record a relative time delay close to 60, because also for this region the distance to the source is higher for Tohoku than for the two Chuetsu events. Regarding the normalized amplitudes, we observe here that the retrograde Rayleigh waves are stronger (relative to the body waves at the central frequencies) for the two Chuetsu events, and that they become weaker in the deepest parts of the basin (in this region).

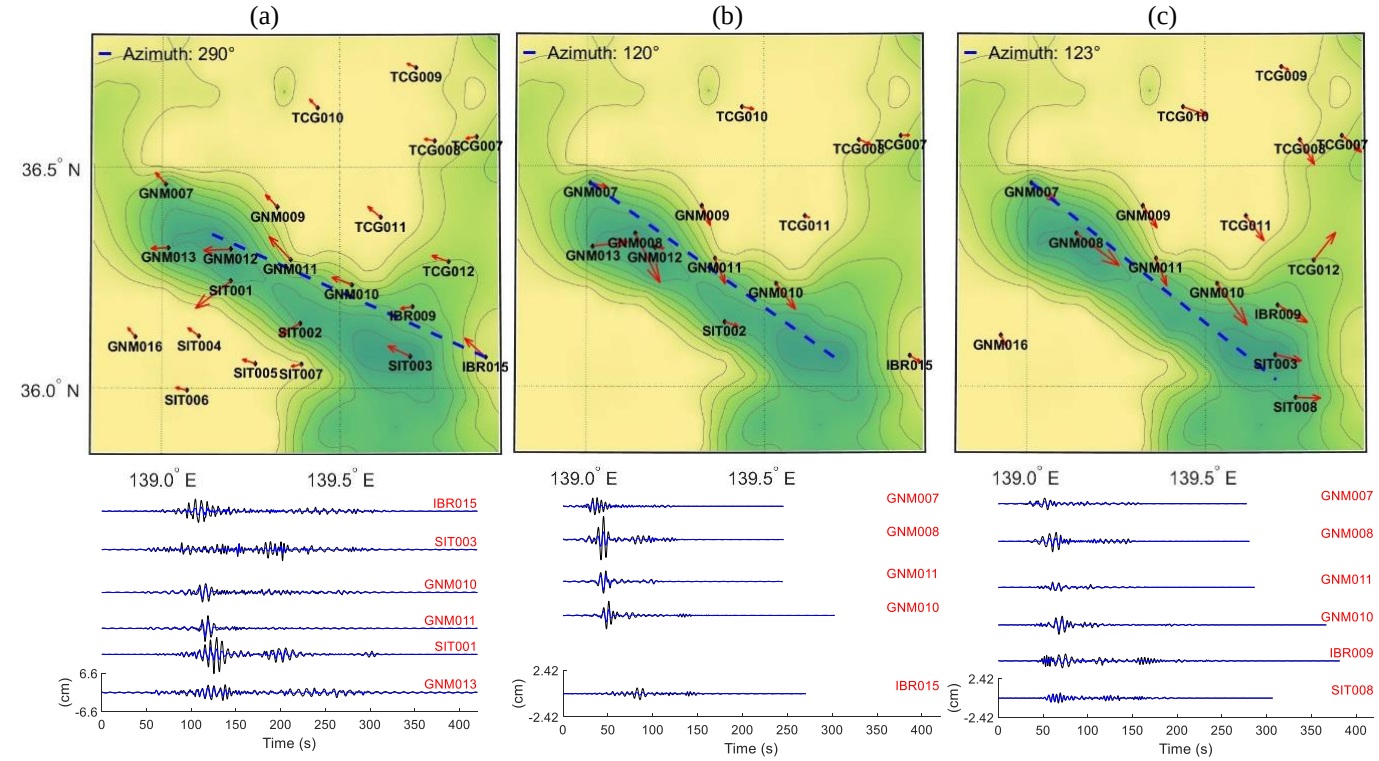

Figure 6. Retrograde Rayleigh waves extracted at the Kanto basin, on the Gunma-Saitama region. During (a) the Tohoku earthquake, (b) the Chuetsu earthquake, (c) the Chuetsu-oki earthquake. Directions of polarization are shown on the top panels. The intermittent straight line indicates the direction of maximum energy averaged over all stations. On the bottom panels, waveforms of horizontal and (shifted) vertical components.

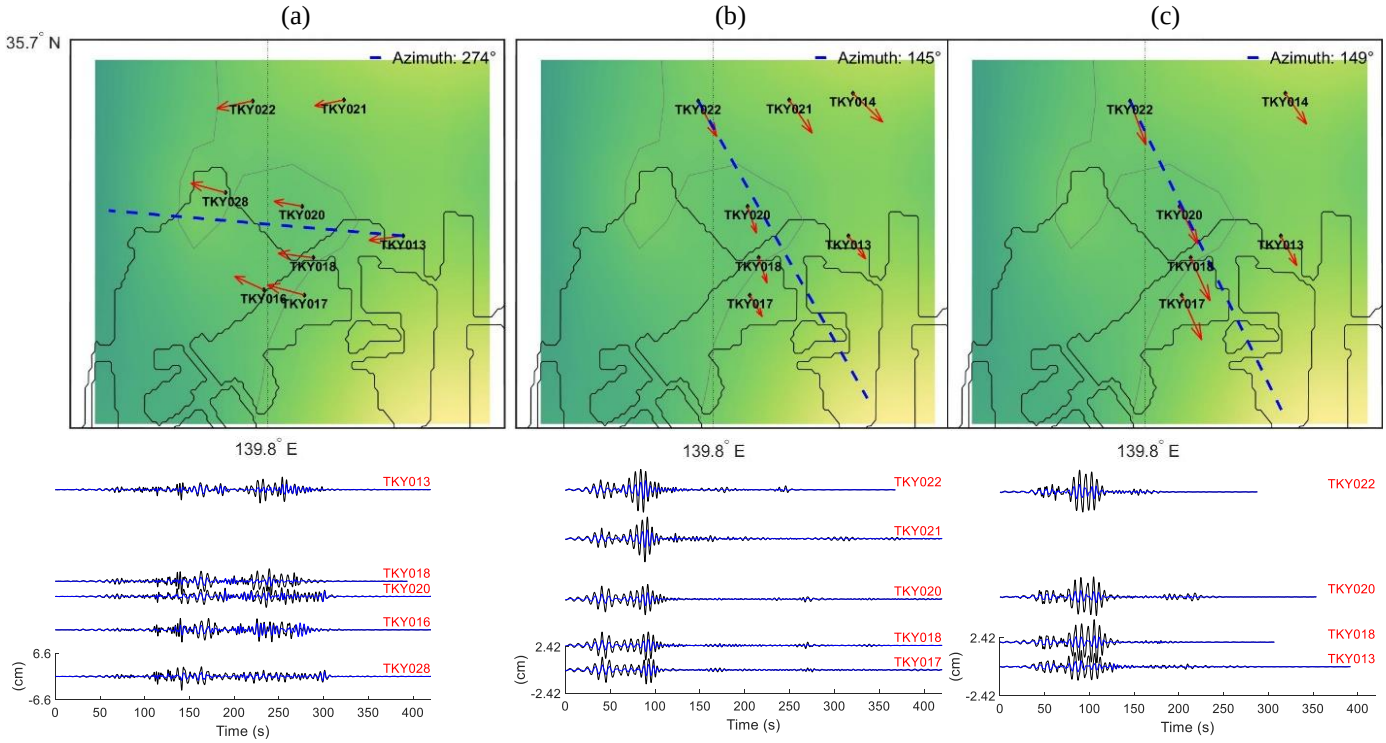

Figure 7. Prograde Rayleigh waves extracted at the Kanto basin, on the Gunma-Saitama region. During (a) the Tohoku, (b) the Chuetsu, (c) the Chuetsu-oki earthquake.

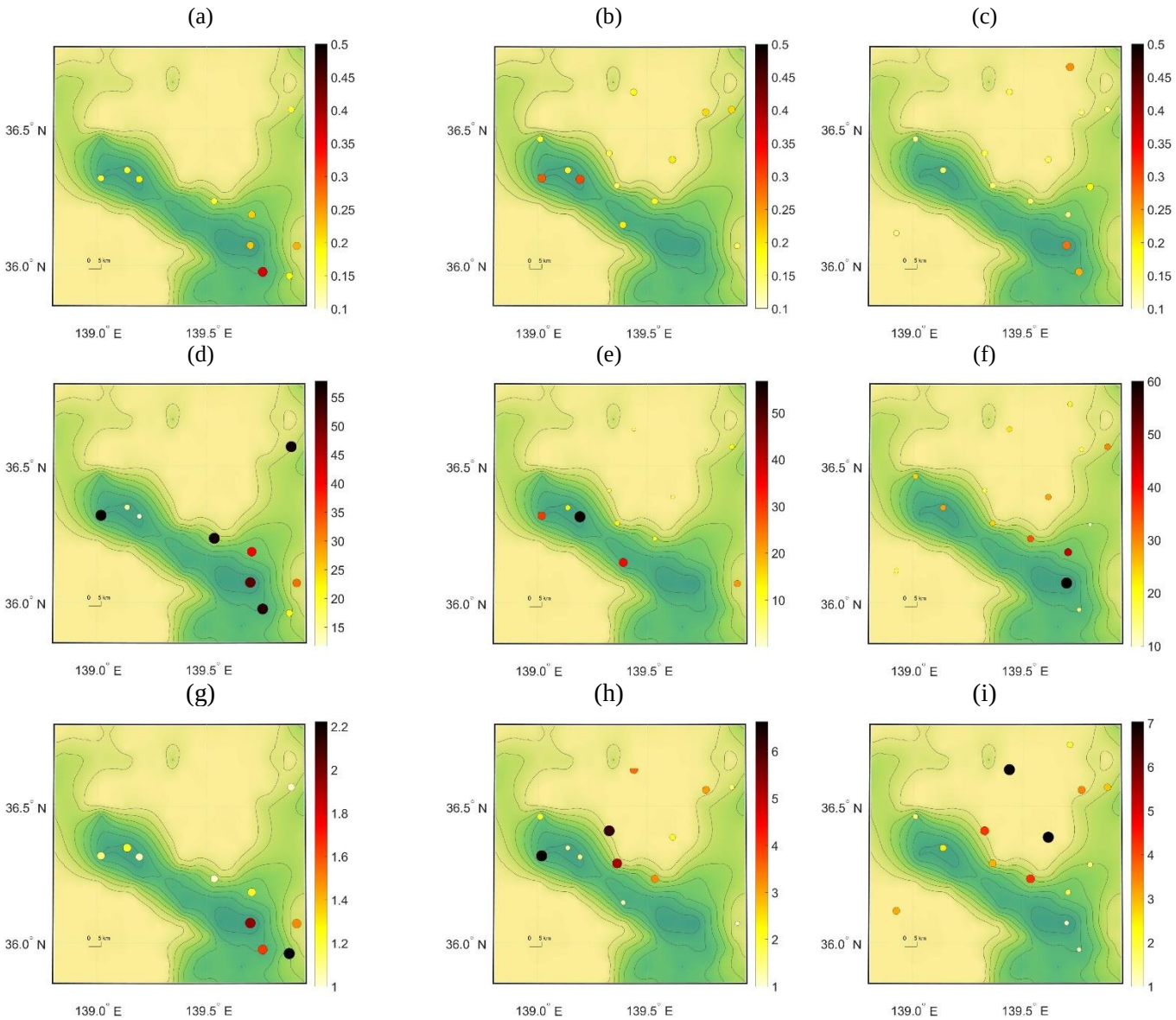

Figure 8. Retrograde Rayleigh waves extracted at the Kanto basin, in the Gunma-Saitama region. (a), (b) and (c) Central frequency (Hz) during the Tohoku, the Chuetsu and the Chuetsu-oki earthquake, respectively. (d), (e) and (f) Relative time delay during the Tohoku, the Chuetsu and the Chuetsu-oki earthquake, respectively. (g), (h) and (i) Normalized amplitude during the Tohoku, the Chuetsu and the Chuetsu-oki earthquake, respectively.

In Figure 9 we show the central frequency with corresponding relative time delay and normalized amplitude of the extracted waves in the Tokyo bay area. In terms of normalized amplitude (relative to the body waves), we observe the lower values (close to 1) during the Tohoku earthquake when compared to the two Chuetsu events, indicating the high intensity of the energy in terms of body waves radiated by Tohoku at low frequencies. For the two smaller events, we observe how the normalized amplitudes diminish as the prograde Rayleigh waves propagate to the southeast. As the extracted waveforms suggest, we find that the relative time delay is longer during the Tohoku earthquake, in a range of 50-110 s, whereas for the two Chuetsu events the range is of 20-45 s. In this region, we attribute this difference to the longer duration of the Tohoku earthquake, during which prograde waves were generated at the basin for a longer time, and thus the most intense wave train arrived at the stations much later. Interestingly, the central frequency of 0.19 Hz of the prograde Rayleigh waves for the two Chuetsu events is consistent in the Tokyo bay area.

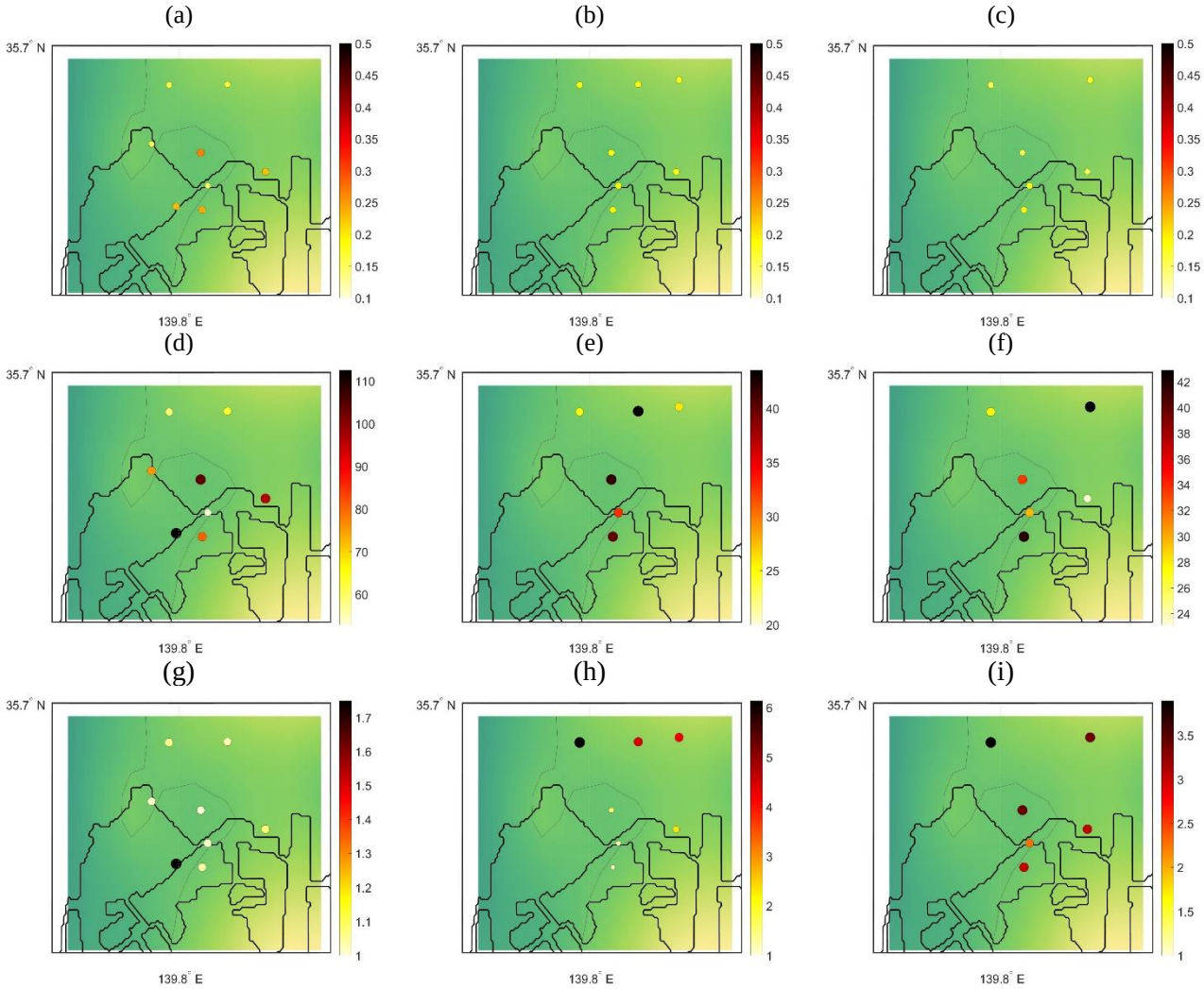

Figure 9. Retrograde Rayleigh waves extracted at the Kanto basin, in the Tokyo bay area. (a), (b) and (c) Central frequency (Hz) during the Tohoku, the Chuetsu and the Chuetsu-oki earthquake, respectively. (d), (e) and (f) Relative time delay during the Tohoku, the Chuetsu and the Chuetsu-oki earthquake, respectively. (g), (h) and (i) Normalized amplitude during the Tohoku, the Chuetsu and the Chuetsu-oki earthquake, respectively.

The last region we analyze in this study is the southeastern Chiba region, where the Kanto basin reaches its largest depth. In this region we also identified *prograde* Rayleigh waves for all three events. The waveforms and directions of propagation are shown in Figure 10, where we can observe how these waves are identified only at stations located on the basin. We can then consider these prograde waves (and the waves identified on the Tokyo bay area) as "*basin generated*". The interstation distances in the Chiba region are larger relative to the Tokyo bay area, and thus the waveforms in Figure 10 are not as coherent as in the Tokyo bay area.

Figure 11 illustrates the central frequency with corresponding relative time delay and normalized amplitude of the extracted waves in the Chiba region. Here we also observe that the central frequency of the prograde waves is about 0.19 Hz, especially at the deepest parts of the basin. The ranges of the relative time delay is similar (10-90 s) for the three events, even though its spatial distribution is more defined for the two Chuetsu events; the longer relative times located in the deeper part of the region. The ranges of normalized amplitude are also similar for the three events, with the highest values on the northern edge of the Chiba sub-basin. At the southern edge we observe the contrary, the values of normalized amplitudes at most stations are very low, between 1 and 1.5. Finally, we find that the amplitude (both absolute and normalized) of the prograde waves is similar to that of the retrograde Rayleigh waves for each of the three events.

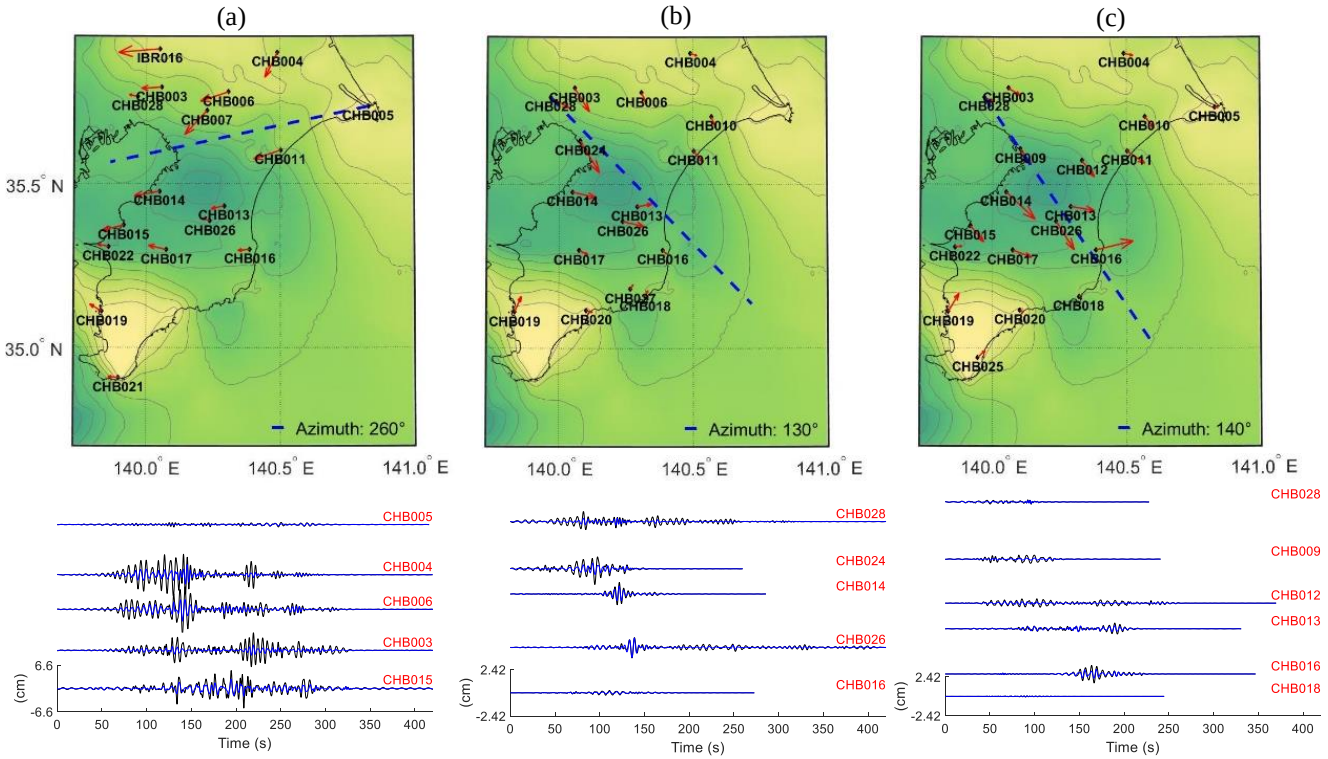

Figure 10. Prograde Rayleigh waves extracted at the Kanto basin, on the Chiba region. During (a) the Tohoku, (b) the Chuetsu, (c) the Chuetsu-oki earthquake.

4. Conclusions

We have identified and analyzed surface waves in the range 0.1-0.5 Hz in the Nobi and the Kanto basin in Japan, registered during the Tohoku, Chuetsu and Chuetsu-oki earthquakes. In order to quantify basin effects we measure the amplitudes of the extracted waves relative to that of the body waves present in the same seismogram. To quantify the dispersive characteristics of surface waves we measure the delay time of central frequency of the extracted waves with respect to the delay time at 3 Hz, a frequency at which we expect to have only non-dispersive body wave energy. Our main conclusions are the following:

1) We identified retrograde low frequency (0.1-0.15 Hz) Rayleigh waves arriving at Nobi during the Tohoku earthquake, which interact with the basin and are diffracted by it. In contrast, we observe that the retrograde Rayleigh waves arriving at Nobi during the two Chuetsu events do not interact with the basin. We attribute this difference to the wider range of azimuthal angles of arriving energy in the frequency range 0.1-0.5 Hz during the Tohoku earthquake. The amplitude of the Rayleigh waves relative to the body waves in the low frequency range is stronger during two Chuetsu events, indicating that Rayleigh waves predominate the time history at that frequency range.

2) Retrograde and prograde Rayleigh waves are observed in the Kanto basin in the range 0.1-0.5 Hz. Conditions favoring the generation of prograde Rayleigh waves include the existence of very soft layers overlying very deep sediments. These conditions apparently exist in the Tokyo lowlands and the deeper parts of the Chiba sub-basin. The central frequency of the identified Rayleigh prograde and Rayleigh waves at most stations in Kanto basin is about 0.19 Hz. The observed amplitudes of prograde and retrograde Rayleigh waves are similar (same order of magnitude).

3) We observe the relative time delay and normalized amplitude of the extracted waves depend strongly on the location and on the size (and therefore duration) of the tectonic source. However, for the

prograde Rayleigh waves in Kanto, that are considered to be "basin generated", other factors such as the depth of the basin and the location of the "generation source" seem to affect these parameters. However, it is imperative that more events need to be analysed to identify patterns of generation/amplification/duration elongation of surface waves to be able to estimate/predict them and synthesize them with confidence.

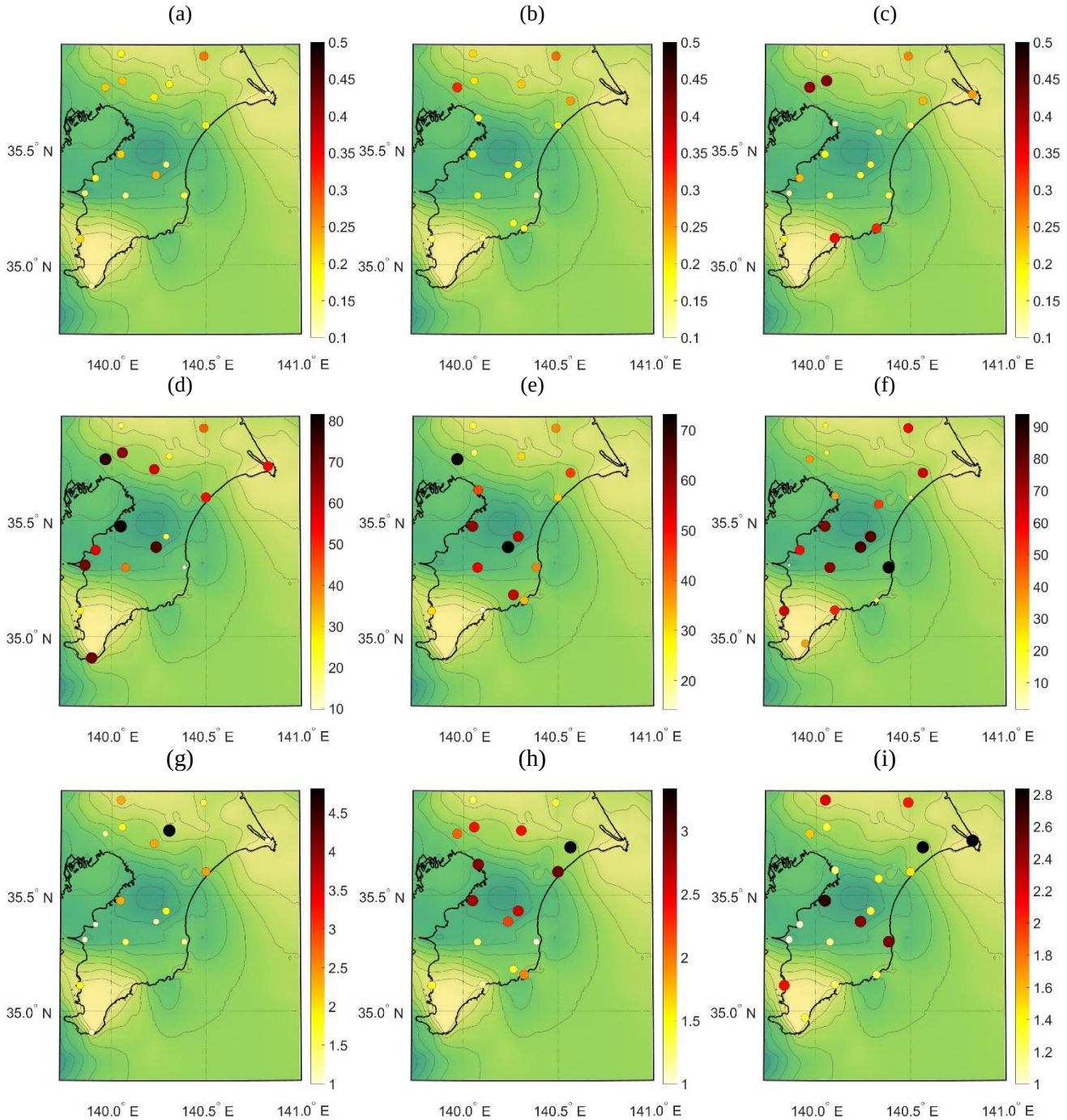

Figure 11. Retrograde Rayleigh waves extracted at the Kanto basin, in the Chiba region. (a), (b) and (c) Central frequency (Hz) during the Tohoku, the Chuetsu and the Chuetsu-oki earthquake, respectively. (d), (e) and (f) Relative time delay during the Tohoku, the Chuetsu and the Chuetsu-oki earthquake, respectively. (g), (h) and (i) Normalized amplitude during the Tohoku, the Chuetsu and the Chuetsu-oki earthquake, respectively.

4. Acknowledgements

This research work has been financed by the French National Research Agency (Agence National de la Recherche), under project MODULATE, grant number ANR-18-CE22-0017. We used the deep subsurface structure data of J-SHIS and K-NET data from NIED, Japan.

6. References

[1] S. Kinoshita, H. Fujiwara, T. Mikoshiba, and T. Hoshino, "Secondary Love waves observed by a strong-motion array in the Tokyo lowlands, Japan," *J. Phys. Earth*, vol. 40, no. 1, pp. 99–116, 1992.

[2] T. Furumura and T. Hayakawa, "Anomalous propagation of long-period ground motions recorded in Tokyo during the 23 October 2004 Mw 6.6 Niigata-ken Chuetsu, Japan, earthquake," *Bull. Seismol. Soc. Am.*, vol. 97, no. 3, pp. 863–880, 2007.

[3] K. C. Meza-Fajardo, A. S. Papageorgiou, and J.-F. Semblat, "Identification and extraction of surface waves from three-component seismograms based on the normalized inner product," *Bull. Seismol. Soc. Am.*, vol. 105, no. 1, 2015.

[4] NIED, "National Research Institute for Earth Science and Disaster Resilience, K-net, Kik-net," 2019.

[5] K. C. Meza-Fajardo and A. S. Papageorgiou, "Estimation of rocking and torsion associated with surface waves extracted from recorded motions," *Soil Dyn. Earthq. Eng.*, vol. 80, 2016.

[6] R. G. Stockwell, L. Mansinha, and R. P. Lowe, "Localization of the Complex Spectrum: The S Transform," *IEEE Trans. Signal Process.*, vol. 44, no. 4, pp. 998–1001, 1996.

